Abstract

Title of the thesis: Structure, Stability, and Interaction of Fibrin αC-Domain Polymers

Ariza Mahid, Master of Science, 2011

Thesis directed by: Leonid Medved Ph.D., Sc.D., Professor, Department of Biochemistry and Molecular Biology, and Center for Vascular and Inflammatory Diseases

Fibrinogen is a multidomain plasma protein that after conversion into polymeric fibrin protects damaged vasculature from blood loss and subsequently participates in wound healing through the interaction of its individual domains with various plasma proteins and cellular receptors. Fibrin(ogen) αC-domains formed by the C-terminal portions of its Aα chains (amino acid residues Aα392-610) play an important role in fibrin assembly, fibrinolysis, and angiogenesis. These domains are inert in fibrinogen and highly reactive in fibrin suggesting that their structure in the latter, in which they form αC polymers, differs from that in fibrinogen. While the structure of the isolated αC-domain has been established, the structure of the αC-domains in fibrin αC polymers remains to be determined. The major goals of the present study were to clarify the structure of fibrin αC-domain polymers and to test our hypothesis that polymerization of the αC-domains results in the exposure of their binding sites. To accomplish these goals, we prepared a recombinant αC region (Aα221-610) including the αC-domain, demonstrated that it forms soluble oligomers in a concentration-dependent and reversible manner, and covalently cross-linked such oligomers with factor XIIIa. Cross-linked Aα221-610 oligomers were stable in solution and appeared as ordered linear arrays when analyzed by electron microscopy. Spectral studies revealed that the αC-domains in such

oligomers were folded into compact structures with significant amount of β-sheets and exhibited high thermal stability. These results indicate that cross-linked Aα221-610 oligomers are highly ordered and mimic the structure of αC polymers in fibrin. Binding studies performed by ELISA and SPR revealed that, in contrast to the monomeric αC-domain, the cross-linked oligomers exhibited prominent binding to tPA and plasminogen indicating that their tPA- and plasminogen-binding sites are exposed. In agreement, these oligomers drastically increased the rate of plasminogen activation in the chromogenic substrate assay. Thus, our study with cross-linked Aα221-610 oligomers clarified the structure of the αC-domains in fibrin αC polymers and confirmed our hypothesis that their binding sites are exposed upon polymerization. Such oligomers represent a stable, soluble model of fibrin αC polymers that can be used for future structural and functional studies of fibrin αC-domains.

Structure, Stability, and Interaction of Fibrin αC-Domain Polymers

By
Ariza Mahid

Thesis submitted to the faculty of the Graduate School of the
University of Maryland, Baltimore in partial fulfillment
of the requirements for the degree of
Master of Science
2011

Table of Contents

List of Figures

I. INTRODUCTION

1. Fibrinogen function

Fibrinogen is a plasma glycoprotein that plays an important role in haemostasis and a number of other physiological and pathological processes. Fibrin(ogen) molecules interact specifically with each other and with a number of proteins and cell types during the execution of various functions [1, 2, 3]. Activation of coagulation cascade leads to the generation of thrombin, which converts soluble fibrinogen into insoluble fibrin polymer resulting in the formation of fibrin-rich blood clot. The clot plugs damaged vessel walls thereby preventing the loss of blood upon vascular injury. Once the haemostatic function is accomplished, the clot is dissolved by degradation with a specific fibrinolytic enzyme plasmin. Polymerized fibrin promotes activation of proenzyme plasminogen into active enzyme plasmin thereby triggering fibrinolysis and subsequently contributes to the propagation of fibrinolysis by keeping plasmin on fibrin surface [4]. Fibrin polymer also serves as a provisional matrix for adhesion, migration and proliferation of cells during the process of wound healing and neovascularization [2]. It promotes physiological inflammation and angiogenesis through specific interactions with a number of leukocyte and endothelial cell receptors [5, 6]. Because of its pro-angiogenic and pro-inflammatory properties and the ability to interact with lipoprotein(a), fibrin(ogen) promotes tumorigenesis and contribute to the development of atherosclerosis. In pathological states, the excessive generation of fibrin leads to thrombosis and the ineffective generation of fibrin predisposes to hemorrhage. This multifunctional character of

fibrin(ogen) is associated with its complex structure that accommodates multiple binding sites providing its participation in the above mentioned processes [7, 8].

2. Fibrinogen structure

Fibrinogen is a 340-kDa chemical dimer consisting of two identical subunits, each of which is formed by three non-identical polypeptide chains, Aα, Bβ, and γ (Figure 1A) [1, 9]. Both the subunits and the chains are linked together by 29 disulfide bonds, and assemble to form more than 20 distinct independently folded domains that were identified by differential scanning calorimetry [10, 11, 12, 13]. These domains are grouped into several structural regions: the central E region, two identical terminal D regions, and two αC regions [7]. The disulfide-linked N-terminal portions of all six chains form the central E region, the C-terminal portions of the Bβ and γ chains and middle portions of the Aα chains form two distal D regions, and the remaining C-terminal portions of the Aα chains form two αC regions. There are also two βN regions, each formed by the N-terminal portion of the Bβ chain [7, 14]. The D-E-D regions account for three nodules, one central E and two terminal D, observed by electron microscopy; a fourth nodule observed in some molecules near the central nodule corresponds to the αC regions [15-19]. The D and E regions are highly resistant to proteolysis and could be prepared by limited digestion of fibrinogen with plasmin and some other proteases [1, 20]. The resultant D and E fragments preserve the compact structure and functional properties of the corresponding regions. In contrast, the αC regions are very susceptible to proteolytic enzymes and are easily degraded into small fragments. Therefore, preparation of a fragment corresponding to these regions is challenging. Previous attempts to prepare full-length αC regions by

limited proteolysis of fibrinogen resulted in a very low yield of truncated fragments and the recovered fragments were missing a significant portion from the COOH-terminus [21, 22].

The crystallographic studies of fibrinogen and its fragments established the three-dimensional structure of more than two-thirds of the fibrinogen molecule. The structure revealed that in each subunit, the Aα, Bβ and γ chains form a triple helical coiled-coil, which links the central globular nodule to the distal globular nodules (coiled coil connector in figure 1B) [7]. According to the crystal structure, the central nodule located in the E region contains two structural domains. Among them, the γN-domain is formed by the N-terminal portions of both γ chains and the funnel-shaped domain is formed by the N-terminal portions of the Aα and Bβ chains [23]. The two distal nodules located in each D region, β-nodule and γ-nodule, are formed by the C-terminal portions of the β and γ chains, respectively. Each of these nodules consists of three crystallographically distinct domains [24, 25]. In addition, each coiled coil connector contains two domains, one in the E region and another one in the D region [23, 24, 26, 27]. Thus, the X-ray studies revealed four structural domains in the central E region and seven structural domains in each D region. The independent folding status of most of these domains has been confirmed by differential scanning calorimetry [10, 11, 12]. Although X-ray studies have established the three-dimensional (3D) structure of the E and D regions, they failed to identify the 3D structure of the βN and αC regions. Therefore, in Figure 1B these regions are shown schematically.

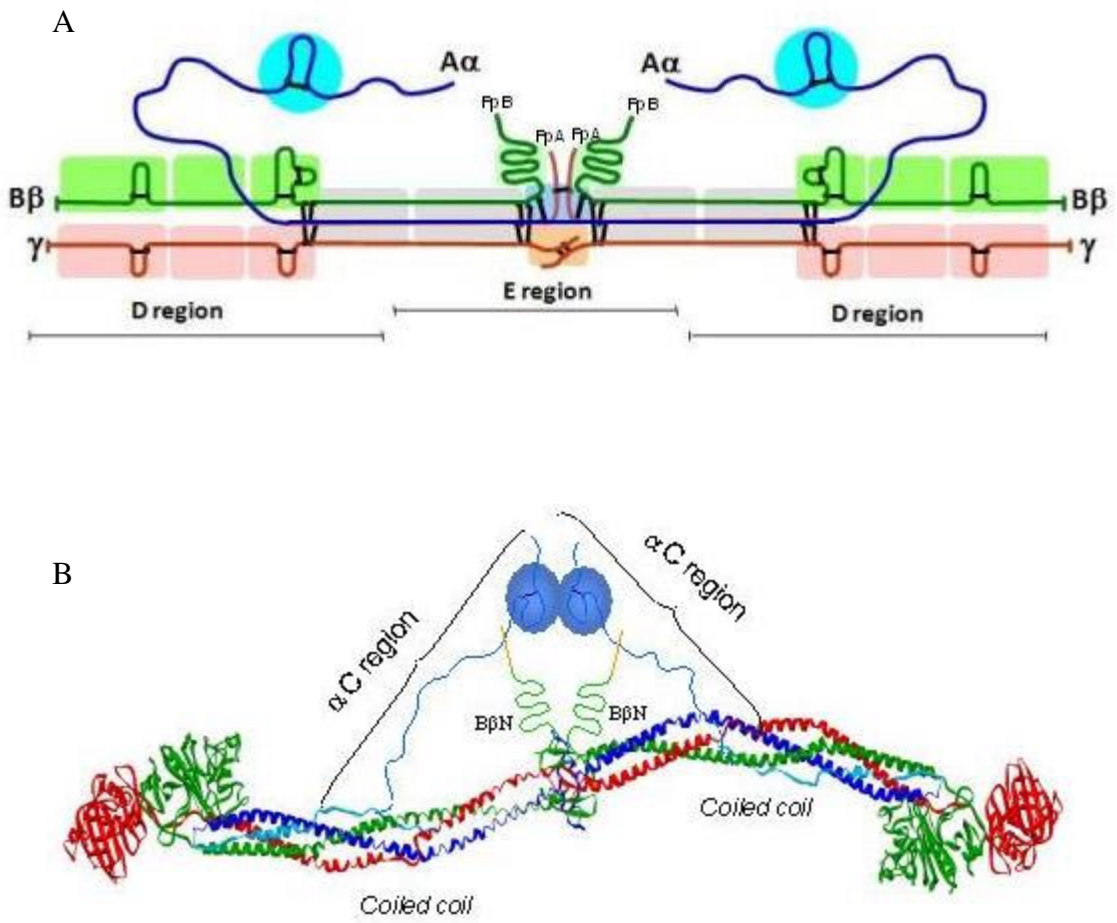

Figure 1. Fibrinogen structure.

(A) Polypeptide chain composition and independently folded domains in fibrinogen [10, 11, 12]. Aα, Bβ, and γ denote individual polypeptide chains, the black bars represent disulfide bonds, FpA and FpB designate fibrinopeptide A and fibrinopeptide B, respectively.

(B) Ribbon model of fibrinogen based upon its crystal structure [27]. The αC regions and N-terminal portions of the Bβ chains (termed as BβN region), whose structure was not identified by X-ray, are shown schematically.

3. Fibrin polymerization

Conversion of soluble monomeric fibrinogen into insoluble polymeric fibrin is mediated by thrombin, a serine protease. Thrombin generated upon activation of the coagulation cascade sequentially cleaves the 16-residue fibrinopeptide A (FpA) and the 14-residue fibrinopeptide B (FpB) from the N-terminal portions of the Aα and Bβ chains, respectively (Figure 1A). These cleavages expose a pair of polymerization sites (knobs) "A" and "B" in the central E region, which include N-terminal sequences Gly-Pro-Arg and Gly-His-Arg, respectively [9]. The knobs "A" and "B" (Figure 2A) interact with complimentary polymerization sites (holes) "a" and "b" located in the distal D regions of adjacent molecules; these interactions play a crucial role in the formation of fibrin polymer [28].

According to the current view, conversion of fibrinogen into fibrin (fibrin assembly) occurs in two major steps. In the first step, the removal of FpA with thrombin enables the "A"-"a" interaction (Figure 2A) leading to the formation of two-stranded protofibrils (Figure 2B). Subsequent removal of FpB in the second step enables the "B"-"b" interaction promoting the lateral association of protofibrils into thicker fibers (Figure 2C) that form a three-dimensional fibrin network, a fibrin clot (Figure 2D) [7, 18]. It was shown that the αC regions also promote lateral association of protofibrils and thereby participate in fibrin assembly [29, 30]. However, there is still no clear understanding on how they contribute to this process.

Factor XIIIa, a specific plasma transglutaminase, covalently cross-links fibrin polymer. This cross-linking stabilizes the structure of fibrin clot. The cross-linking

(formation of a covalent bond) occurs between reactive glutamine (Gln) and lysine (Lys) residues located in the γ-nodules (γ-γ cross-linking) and the αC regions (α-α cross-linking) [31]. In fibrin, the γ-γ cross-linking between two adjacent γ-nodules occurs very rapidly. It starts at the stage of protofibril formation and results in the formation of γ-γ dimers. The α-α cross-linking is more complicated and occurs more slowly resulting in the formation of αC polymers (Figure 2C) [31]. Both types of covalent cross-linking contribute to the stability of fibrin.

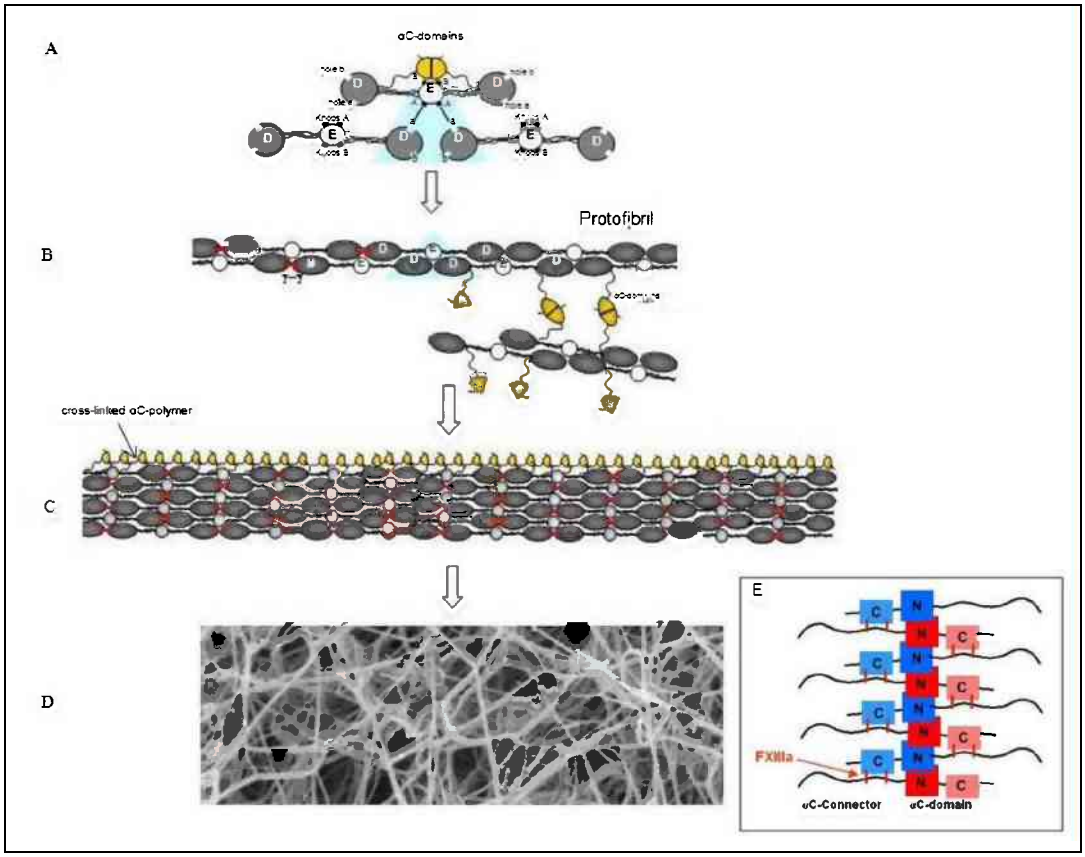

Figure 2: Fibrin assembly process.

Panel A shows "A"-"a" interaction between three molecules leading to the formation of two-stranded protofibrils shown in panel B. The protofibrils laterally associate to form thicker fibers (panel C), which form three-dimensional fibrin network (panel D) [32]. In panel A, two interacting αC-domains are shown only in the upper molecule; D and E represent the terminal D regions and central E region, respectively; the intermolecular interaction between the αC-domains of neighboring molecules is shown in panel B; the γ-γ cross-linking is shown by red bars in panel B and C. αC polymers formed by intermolecular interaction between the αC-domains and cross-linked by factor XIIIa are shown in panel C; panel E shows a possible arrangement of the αC-domains in fibrin αC polymers.

4. Structure and function of the αC-domains in fibrinogen and fibrin

The structural organization of the αC-regions was extensively studied by various methods. Electron microscopy of individual fibrinogen molecules revealed the presence of an extra nodule adjacent to the central nodule; however, this extra nodule was absent in the truncated fibrinogen missing the C-terminal portions of Aα chains (termed as X fragment) [17, 19]. Thus, it was suggested that this nodule is made up of the two αC regions [19]. Differential scanning calorimetry of fibrinogen and its fragment X revealed an extra heat absorption peak in the endotherm of the fibrinogen molecule in comparison to its X fragment in which the corresponding peak was absent [10]. Therefore, this peak was assigned to melting of the αC regions [10]. A detailed analysis of this peak revealed that the two αC regions form two compact cooperative units that strongly interact with each other [12]. However, X-ray studies of intact fibrinogen failed to establish the 3D structure of the αC regions resulting in conclusion that these regions are unordered or natively unfolded [27, 33].

To further clarify the structural organization of the αC region, a fragment corresponding to this region, Aα221-610, and its sub-fragments, Aα221-391, and Aα392-610, corresponding to the N-terminal and C-terminal halves, respectively, were expressed in bacterial system, refolded, and their structure was characterized by fluorescence spectroscopy and circular dichroism [13]. The study revealed that each αC region consists of two structurally distinct portions. Namely, the C-terminal half of the αC region (residues Aα392-610) is folded into a compact structure termed αC-domain while the N-terminal half (residues Aα221-391) forms a flexible tether connecting this domain to the

bulk of the molecule; this tether was termed the αC-connector (Figure 1B) [13]. Recent studies with the recombinant human and bovine fibrinogen αC-domain fragments established that each αC-domain consists of two independently folded units termed N-terminal sub-domain and C-terminal sub-domain (Figure 3A) [34]. The 3D solution structure of the N-terminal sub-domain of the bovine fibrinogen αC-domain (bAα406-483 fragment) has been established earlier by NMR [35]. According to the structure, this sub-domain contains a parallel/antiparallel β-sheet consisting of two β-hairpins (Figure 3B). The overall fold of the N-terminal sub-domain of the human fibrinogen αC-domain (hAα425-503 fragment) was shown to be similar (Figure 3C) [34].

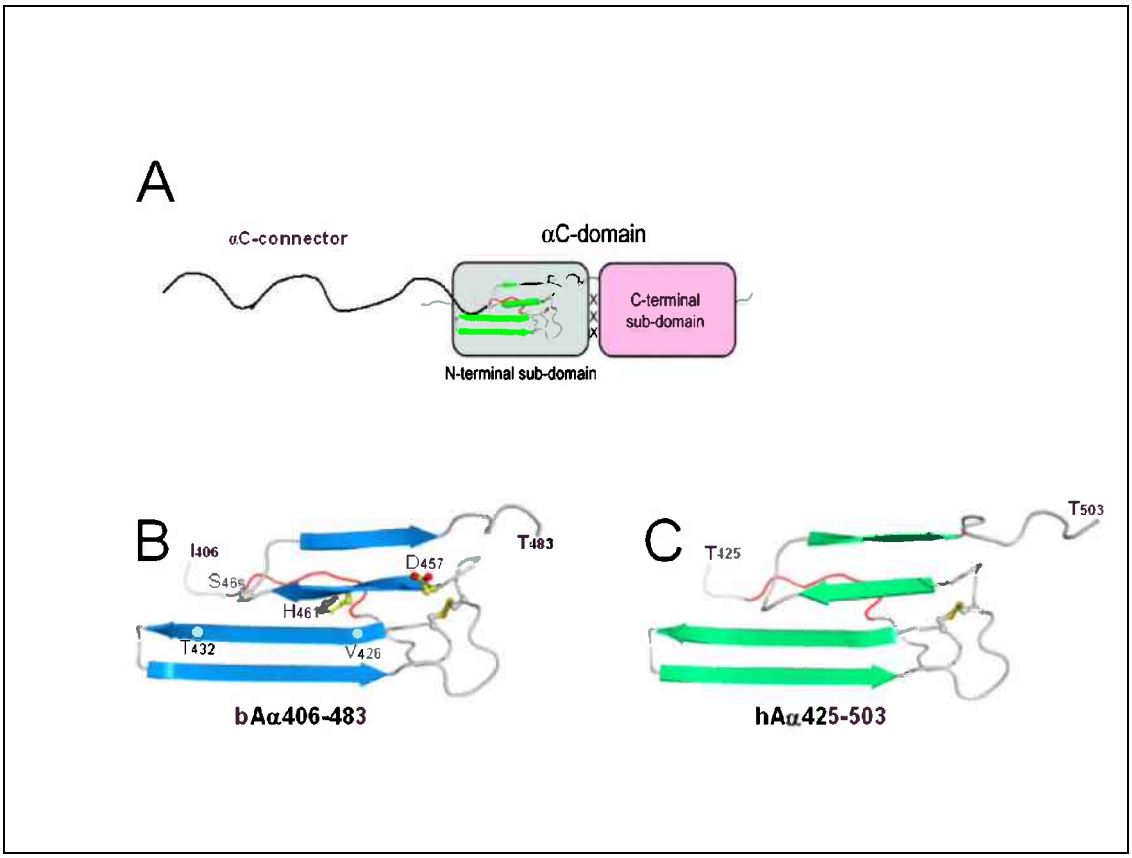

Figure 3. Structural organization of the fibrinogen αC-domain.

(A) Schematic representation of the αC-domain containing N-terminal and C-terminal sub-domains; the three X represent the interaction between these domains; the αC-connector is also shown [34].

(B) Ribbon diagram of the bovine bAα406-483 fragment based upon its NMR structure [35]. Arrows indicate β-strands, and the region of slower motion is colored red.

(C) Homology model of the human hAα425-503 fragment built based on the 3D structure of bovine bAα406-483 [34].

Numerous studies suggest that in fibrinogen the αC-domains interact intramolecularly with each other to form a dimer, which, in turn, interacts with the central E region, while in fibrin they form αC polymers (Figure 2A and C). These polymers are stabilized by covalent cross-linking with activated factor XIII (factor XIIIa) and can be easily identified by analyzing cross-linked fibrin using SDS-PAGE in reduced conditions [1]. It was shown that the cross-linking occurs between reactive Lys residues of the αC-domain and reactive Gln residues of the αC-connector. Namely, Lys508, 539, 556, 580 and 601 located in the C-terminal sub-domain of the αC-domain and Gln221, 237, 328, and 366 of the αC-connector are involved in the cross-linking [36, 37, 38]. This cross-linking alters the mechanical properties of the fibrin clot and enhances clot's resistance to lysis by plasmin [39]. Thus, the structure of the αC-domains in fibrinogen and fibrin seems to be different. While the structure of the isolated αC-domain has been established, that of the αC-domains in fibrin αC polymers remains to be clarified.

According to the proposed hypothesis [29, 30, 40], upon fibrin assembly, the αC-domains switch from intra- to intermolecular interactions resulting in the formation of αC polymers. This hypothesis suggests a possible mechanism for formation of αC polymers; however, it was not widely accepted due to lack of direct experimental evidence. A recent study with a recombinant fragment corresponding to the N-terminal sub-domain of the αC-domain found that this fragment can self-associate and form soluble oligomers in a concentration-dependent manner [35]. It was also shown that the oligomerization increases the thermal stability of the fragment [35]. Similar results were obtained in a subsequent study conducted with the recombinant full-length αC-domain, which confirmed formation of reversible oligomers by this domain and their thermal

stabilization [34]. Based on these and some other studies, it was hypothesized that oligomerization of the recombinant αC-domain may mimic polymerization of the αC-domains in fibrin and the structure of αC oligomers may mimic that of fibrin αC polymers [34, 35]. Further studies of oligomers formed by the recombinant αC-domain are required to test this hypothesis.

The αC domains contain a number of binding sites and participate in the regulation of various fibrin(ogen) activities. As mentioned earlier, they promote lateral association of protofibrils during the process of fibrin assembly [30]. In addition to fibrin assembly, they participate in controlling the activation of factor XIIIa [41], which subsequently cross-links the αC regions thereby contributing to the mechanical stability of fibrin clot. The αC-domains promote cell adhesion via their Aα572-574 RGD sequence and via bound fibronection [42, 43]. They also contain binding sites for plasminogen and its activator, tPA, and inhibitor, α_2-antiplasmin [44, 45], and thus play a prominent role in regulation of fibrinolysis. Numerous studies revealed that fibrinogen from which the αC-domains are removed by limited proteolysis or recombinant techniques exhibits retarded polymerization and altered architecture of fibrin clots; fibrinolysis of such clots are also altered [46, 47, 48]. Congenital defects in the αC-domains alter fibrin polymerization and clot structure and cause severe pathological consequences including familial recurrent thrombosis, pulmonary embolism, and hemorrhage [49, 50, 51]. It was also reported that several naturally occurring mutations in the αC-domain cause renal amyloidosis [52-55].

Although the fibrin αC-domains are highly reactive towards various proteins and cell types, they seem to be inert in fibrinogen [44, 45, 56, 57]. Several experiments

conducted in our laboratory found that none of the proteins containing αC-domain binding sites, tPA, plasminogen, apolipoprotein(a), fibronectin, α_2-antiplasmin, interacted with either highly purified fibrinogen or the isolated αC-domains kept in solution. These interactions were observed only when fibrinogen was converted into fibrin, or when the αC-domains or fibrinogen were immobilized onto the surface [44, 45, 56, 57]. *These observations led us to hypothesize that numerous binding sites in the αC-domains are cryptic in fibrinogen and become accessible in fibrin. This implies that the αC-domains undergo conformational changes upon conversion of fibrinogen into fibrin, and that only in polymeric fibrin they adopt the physiologically active conformation.* Testing this hypothesis would require comparison of the structure and binding properties of the fibrinogen αC-domains with those of fibrin αC-domains. This is challenging since the αC-domains represent only a portion of fibrin(ogen) and most of the αC-domain ligands also interact with other fibrin(ogen) domains. To overcome this challenge, a soluble model mimicking the structure and function of the αC-domains in fibrin is required.

II. GOALS AND OBJECTIVES

The major goals of the present study were to elucidate the structure of the αC-domains in polymeric fibrin and to prove that the binding sites of the αC-domains are exposed upon their polymerization.

The objectives of the study were to:

1) Create and prepare a soluble model of fibrin αC-domain polymers

2) Characterize the structure of the αC-domains in this model by various methods

3) Using this model, test the hypothesis that cryptic binding sites of the αC-domains are exposed upon conversion of fibrinogen into fibrin

III. MATERIALS AND METHODS

1. Proteins and antibodies

Plasminogen-depleted human fibrinogen, human α-thrombin, human Glu-plasminogen and human factor XIIIa were purchased from Enzyme Research Laboratories. Bovine serum albumin was purchased from Thermo Scientific. Recombinant single-chain tPA was a Genentech product. The monoclonal antibody TF 359/1-1 directed against the αC region was a gift from Dr. B. Kudryk (New York Blood Center, New York). The alkaline phosphatase conjugated ExtrAvidin was purchased from Sigma.

2. Preparation of recombinant fragments

A recombinant Aα221-610 fragment corresponding to the human fibrinogen αC region was expressed in *E. coli* B834 host cells using pET-20b expression vector. The plasmid constructed and described earlier [44] was used to transform the *E. coli* cells. In the process of transformation, 1 µl plasmid at the concentration of 5 ng/µl was added to the B834 (DE3) pLysS cell and incubated on ice for 15 min. The reaction mixture was heat shocked at 42 ^{0}C for 43 sec, incubated on ice for 5 min followed by incubation with SOC media at 37 ^{0}C for 1 hour to recover the cells. 50 µl of the cells were spread on a Luria Broth (LB) plate containing 50 µg/ml of carbenicillin and incubated inverted at 37 ^{0}C overnight for growing the colonies.

For expression of the Aα221-610 fragment, one bacterial colony from the agar plate was added to the LB medium containing 50 µg/ml of carbenicillin and allowed to grow the culture overnight with shaking at 37 ^{0}C. Overnight culture was diluted 1:200 with fresh LB medium and allowed to grow with vigorous shaking at 37 ^{0}C until the optical density reached 0.6. The expression was induced by adding 0.4 mM isopropyl-1-thio-β-D-galactopyranoside (IPTG) and incubating for 3 hours at 37 ^{0}C with continuous shaking. The cells were harvested by centrifugation at 4,500 rpm for 10 min, resuspended in 20 mM Tris buffer, pH 7.4, containing 0.15 M NaCl (TBS) and frozen at –20 ^{0}C.

The cells were lysed by freeze/thaw method, then incubated with 200 u/ml of recombinant Dnase by constant stirring at room temperature for 3-4 hours to degrade DNA contaminants, and centrifuged at 12,000 rpm for 20 min to separate the pellet containing insoluble inclusion bodies. The inclusion bodies were washed three times with TBS containing 5 mM EDTA and 0.5% triton X-100 to remove *E. coli* membrane proteins. The inclusion bodies were then dissolved in 8 M urea adjusted to pH 7.4 with 20 mM Tris-HCl and centrifuged to remove residual insoluble material. The soluble Aα221-610 fragment obtained from inclusion bodies was further purified by size-exclusion chromatography on Superdex 200 equilibrated with 4 M urea. The purity and integrity of the fragment was confirmed by SDS-PAGE (Figure 4).

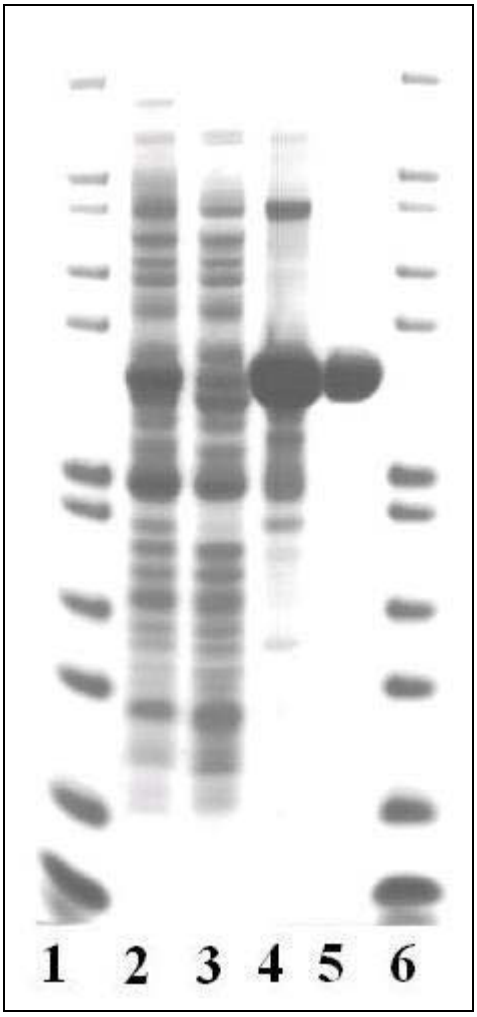

Figure 4: SDS-PAGE analysis of different stages of purification of the expressed Aα221-610 fragment.

Lane 1 and 6 contain molecular mass standards; lane 2, 3, and 4 represent total cell lysate, soluble fraction, and insoluble fraction containing inclusion bodies, respectively; lane 5 shows the Aα221-610 fragment after final purification by size-exclusion chromatography. The electrophoresis was performed in reduced conditions.

The purified Aα221-610 fragment was refolded by slow dialysis from urea at 4 ^{0}C. For refolding, the protein was diluted with 8 M urea to a final concentration of 10 μM. Then the concentration of urea in the container was slowly reduced to 0.8 M by addition of 20 mM Tris buffer, pH 7.4, containing 2 M NaCl overnight at 4 ^{0}C. The concentration of urea was further reduced to 0.08 M by slow dialysis overnight at 4 ^{0}C versus TBS. The refolded fragment was separated from unfolded material by size-exclusion chromatography performed at 4 ^{0}C on a Superdex 200 column equilibrated with TBS at the flow rate of 0.5 ml/min. The refolded Aα221-610 fragment was stored at 4 ^{o}C.

A recombinant Aα392-610 fragment corresponding to the human fibrinogen αC-domain was expressed in *E. coli* B834 (DE3) pLysS host cells using pET-20b expression vector constructed and described earlier [44]. This fragment was found predominantly in inclusion bodies and was purified and refolded following the aforementioned procedures except that the purification was carried out on Superdex 75 column equilibrated with 4 M urea or TBS.

3. Size-exclusion chromatography

Analytical size-exclusion chromatography was used to analyze the aggregation state of the prepared recombinant Aα221-610 fragment. The experiments were performed with a fast protein liquid chromatography system (FPLC, Pharmacia) on Superdex 200 column at the flow rate of 0.5 ml/min. Typically, 500 μl of the fragment was loaded onto the column equilibrated with TBS or 20 mM Tris buffer, pH 7.4, containing 2 M NaCl

and eluted with the same buffer. The elution was monitored by measuring absorbance at 280 nm.

4. Transmission electron microscopy

Soluble cross-linked Aα221-610 oligomers or monomeric Aα221-610 fragment was diluted in a volatile buffer containing 50 mM ammonium formate, pH 7.4, and 30% glycerol to a final concentration of 40 μg/ml. The samples were sprayed onto freshly cleaved mica and rotary shadowed with tungsten in a vacuum evaporator, as previously described [21]. The samples were examined in a Phillips 400 electron microscope at 80 kV and 60,000x magnifications by our collaborators Dr. Y. Veklich and Dr. J. Weisel (University of Pennsylvania School of Medicine).

5. Circular dichroism

Circular dichroism (CD) measurements were performed with a Jasco-810 spectropolarimeter. CD spectra of cross-linked Aα221-610 oligomers, monomeric Aα221-610, and Aα392-610 oligomers were recorded using a 0.01 cm path length quartz cuvette. The measurements were taken in TBS at 4 ^{0}C; fragments concentration was 0.5-1.0 mg/ml. Analysis of the CD spectra was performed using the secondary structure prediction program supplied with the spectropolarimeter, which is based on the previously published method [58]. All CD data were expressed as the mean residue ellipticity, [θ], in units of degrees square centimeter per decimole.

6. Fluorescence spectroscopy

Fluorescence measurements of thermal-induced unfolding of the cross-linked and non cross-linked Aα221-610 oligomers, and monomeric Aα221-610 were performed in an SLM 8000-C fluorometer. The fluorescence intensity ratio at 370 nm to that at 330 nm was monitored with excitation at 280 nm. Temperature was controlled with a circulating water bath programmed to raise the temperature at 1 ^{0}C/min. The concentration of the oligomers was measured spectrophotometrically and was kept at about 0.05 mg/ml. The fluorescence study was carried out in TBS as well as in 20 mM Tris buffer, pH 7.4, containing 2 M NaCl.

7. Enzyme-linked immunosorbent assay

Enzyme-linked immunosorbent assay (ELISA) was performed to test if cryptic binding sites were exposed in soluble cross-linked αC-oligomers. Two αC-domain ligands, tPA and plasminogen, were used for these experiments. Microtiter Immulon 2HB plate (Thermo Scientific) wells were coated overnight with 100 µl/well of tPA and plasminogen at the concentration of 5 µg/ml in TBS containing 1 mM $CaCl_2$; the control wells were left empty. All wells including the control ones were washed three times with TBS containing 1 mM $CaCl_2$ and 0.01% tween-20 (TBS-Ca-Tw) and then incubated with 1% BSA in the same buffer at 37 ^{0}C for one hour to block any non-specific binding. Non-bound BSA was removed by washing three times with TBS-Ca-Tw buffer. 1 µM of cross-linked Aα221-610 oligomers, monomeric Aα221-610, or fibrinogen was added to the wells coated with plasminogen or tPA and also to the control wells and incubated for

one hour at 37 ^{0}C. The wells were then washed three times with TBS-Ca-Tw buffer. Biotinylated anti-Aα221-610 monoclonal antibody TF 359/1-1 was added to each well and incubated at 37 ^{0}C for one hour followed by washing three times with TBS-Ca-Tw buffer. Bound αC-fragments were detected by reaction with the biotinylated TF 359/1-1 monoclonal antibody and the alkaline phosphatase-conjugated avidin. An alkaline phosphatase substrate, PNPP (p-nitrophynyl phosphate disodium salt) was added to the wells and the amount of bound ligand was measured spectrophotometrically at 405 nm.

8. Surface plasmon resonance

The interaction of plasminogen and tPA with cross-linked Aα221-610 oligomers and Aα221-610 monomer was studied by surface plasmon resonance (SPR) using the BIAcore 3000 biosensor (Biacore AB, Uppsala, Sweden), which measures association/dissociation of proteins in real time. In the first set of experiments, tPA or plasminogen in 10 mM sodium acetate, pH 4.5, at 5 µg/ml were covalently coupled to the activated surface of CM5 biosensor chip according to the manufacturer instructions, cross-linked Aα221-610 oligomers, Aα221-610monomer, or fibrinogen at 1 µM or 2 µM were injected, and their association/dissociation was monitored in real time. In the second set of experiments, Aα221-610 monomer and cross-linked Aα221-610 oligomers, both at 5 µg/ml in 10 mM sodium acetate, pH 4.5, were immobilized onto the surface of a sensor chip, increasing concentrations of plasminogen or tPA (from 0 to 1000 nM) were injected, and their association/dissociation was monitored.

Binding experiments were performed in 20 mM HEPES, pH 7.4, with 150 mM NaCl, 1 mM $CaCl_2$, and 0.01% Tween-20 (binding buffer) at 20 µl/min flow rate. The

association between the immobilized ligands and the added analytes was monitored as the change in the SPR response. The dissociation of the complex was initiated by substitution with the binding buffer lacking analyte and monitored in the same manner. For regeneration of the chip surface, bound analyte was removed by adding 0.1 M ε-aminocapronic acid in binding buffer for 30 sec following re-equilibration with the binding buffer. Experimental data were analyzed using BIAevaluation 4.1 software supplied with the instrument. The dissociation equilibrium constant, $K_{d,}$ was calculated as $K_d = k_{diss}/k_{ass}$. The association rate constant (k_{ass}) and the dissociation rate constant (k_{diss}) were estimated by global analysis of the association/dissociation data using the 1:1 Langmurian interaction model (kinetic analysis). To confirm the kinetic analysis, K_d was also estimated by analysis of the association data using the steady-state affinity model provided by the same software (equilibrium analysis).

9. Chromogenic substrate assay

The stimulating effect of cross-linked Aα221-610 oligomers, cross-linked Aα221-610 monomer, monomeric Aα221-610, and fibrinogen on the tPA catalyzed conversion of plasminogen into plasmin was evaluated by measuring the amidolytic activity of the newly formed plasmin with the chromogenic substrate S-2251 (H-D-valyl-L-leucyl-L-lysine-p-nitroanilide). The assay was carried out at 37 ^{0}C. The assay system contained 200 nM plasminogen, 0.14 nM tPA, 0.3 mM S-2251, and 0.5 μM Aα221-610 oligomers, Aα221-610 monomer, or 0.25 μM fibrinogen in TBS, pH 7.4, with 0.05% Tween-80. The amidolytic activity was determined by measuring the change in absorbance at 405 nm using VERSAmax 96-well plate reader (Molecular Devices).

IV. RESULTS

1. Search for conditions for oligomerization of the Aα221-610 fragment

Since the recent study established conditions for reversible ordered oligomerization of the isolated αC-domain (amino acid residues Aα392-610) [34], we hypothesized that the recombinant full-length αC region (Aα221-610) would also form ordered oligomers when subjected to similar conditions. However, such Aα221-610 oligomers could be unstable due to dissociation upon lowering their concentration, as was the case with Aα392-610 oligomers [34]. Therefore, we assumed that they could be stabilized by covalent cross-linking with activated factor XIII (factor XIIIa) since Aα221-610 includes the αC-connector (Aα221-391) to which the αC-domain is normally cross-linked in fibrin αC polymers.

To test the above hypothesis, we studied aggregation state of Aα221-610 by size-exclusion chromatography at two different concentrations. The refolded and purified Aα221-610 fragment was incubated for two days in TBS at 1 mg/ml and 3 mg/ml and size-exclusion chromatography on Superdex 200 column equilibrated with TBS was performed at 4 ^{0}C. The experiments revealed that the fragment was preferentially monomeric at 1 mg/ml, while at 3 mg/ml about 22% Aα221-610 formed oligomers. When the sample containing oligomers was diluted 3-fold, from 3 mg/ml to 1 mg/ml, and immediately analyzed by size-exclusion chromatography, the amount of oligomers dropped to 18%. Subsequent incubation of the diluted sample (1 mg/ml) for one day resulted in further reduction of oligomeric fraction to 11%. Thus, these experiments indicate that like Aα392-610, the Aα221-610 fragment forms reversible soluble

oligomers in a concentration-dependent manner. This suggests that the interaction between individual fragments upon oligomerization is highly specific and that the oligomers are ordered and may mimic those in fibrin.

To test the assumption that Aα221-610 oligomers could be stabilized by covalent cross-linking with factor XIIIa we performed the following experiments. The oligomeric and monomeric fractions of Aα221-610 incubated in TBS were collected, concentrated to 0.9 mg/ml, incubated with 40 μg/ml of factor XIIIa, 1.25 u/ml of thrombin, and 5 mM $CaCl_2$ for varying times and the time course of their cross-linking was analyzed by SDS-PAGE. The time points used for cross-linking were 5, 15, 30, 45 and 90 min with 0 min as a control. The SDS-PAGE analysis revealed that most of the Aα221-610 oligomers (band 1, b1) were rapidly cross-linked intermolecularly resulting in dimers, trimers, tetramers and larger multimers (Figure 5A). These species were also observed upon cross-linking of Aα221-610 monomer; however, their cross-linking was much slower (Figure 5B). In addition, a large portion of the monomer was converted into a species with higher mobility (band 2, b2), which was previously described as the intramolecularly cross-linked monomeric Aα221-610 fragment [36], and the amount of multimers was much lower.

Although SDS-PAGE analysis confirmed that Aα221-610 oligomers are cross-linked more efficiently than the monomer, the yield of the oligomers after incubation in TBS was quite low (about 22%). To further increase the yield of the oligomers and optimize the conditions for their cross-linking, the amount of NaCl in TBS was increased to a final concentration of 2 M since the previous studies of the recombinant αC-domain and its truncated fragments showed increased oligomerization at this NaCl concentration

[34, 35]. The refolded Aα221-610 at 3 mg/ml was incubated overnight in TBS containing 2 M NaCl and then analyzed by size-exclusion chromatography. The experiments revealed that the amount of oligomers was about 60%, i.e. much higher than that revealed after incubation of this fragment in TBS. The oligomers were separated from the monomer by size-exclusion chromatography on Superdex 200, concentrated to 0.5 mg/ml, and cross-linked with factor XIIIa as described above. The separation and cross-linking were performed in the presence of 2 M NaCl to maximally reduce dissociation of the oligomers. The lower concentration of oligomers in this case was used to further reduce the intramolecular cross-linking between monomers that may have been present in the reaction mixture due to slow dissociation of the oligomers. SDS-PAGE analysis of the cross-linking process (Figure 5C) revealed a cross-linking pattern similar to that observed in TBS (Figure 5A). However, the yield of oligomers upon incubation of Aα221-610 in 2 M NaCl was much higher compared to that upon incubation in TBS.

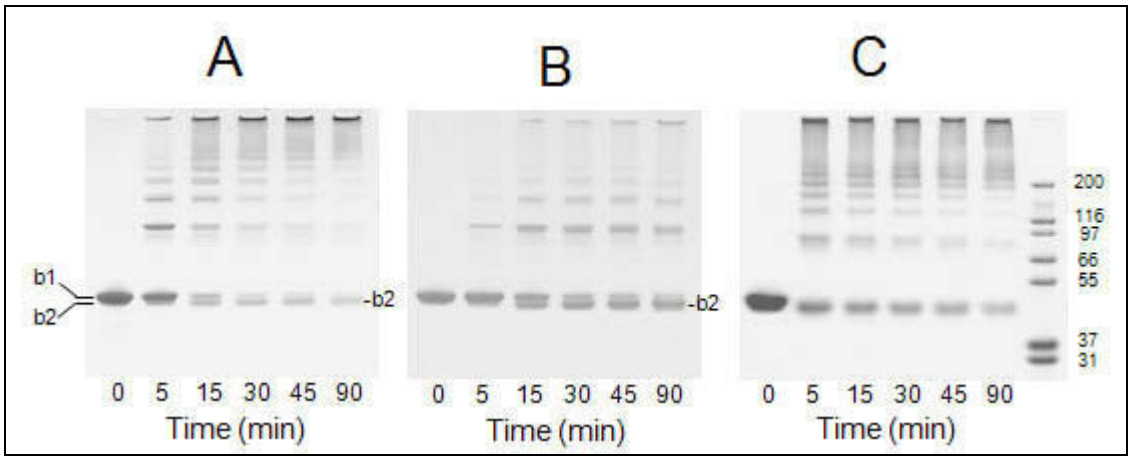

Figure 5: Time-course of cross-linking of Aα221-610 oligomers and Aα221-610 monomer by activated factor XIII.

Panel A and B represent time-course of cross-linking of Aα221-610 oligomers and Aα221-610 monomer, respectively, in 20 mM Tris, pH 7.4, with 0.15 M NaCl (TBS) and 5 mM $CaCl_2$ at room temperature. Panel C represents time-course of cross-linking of Aα221-610 oligomers by activated factor XIII in 20 mM Tris, pH 7.4, with 2 M NaCl and 5 mM $CaCl_2$, at room temperature; the right outer lane contains protein markers of the indicated molecular masses.

2. Preparation of soluble cross-linked Aα221-610 oligomers

Based on the above results, for large-scale preparation, purified and refolded Aα221-610 at 3 mg/ml was incubated overnight in 2 M NaCl at 4 ^{0}C. The oligomers were collected by size-exclusion chromatography on Superdex 200 column equilibrated with TBS containing 2 M NaCl and then cross-linked in the same buffer using conditions described above. The cross-linking reaction was stopped after 30 min by the addition of 10 mM EDTA, the non-soluble material was removed by centrifugation, and the soluble mixture was fractionated on Superdex 200 column equilibrated with TBS. The fractionation was carried out at 4 ^{0}C with a flow rate of 0.5 ml/min. The elution profile exhibited two poorly resolved peaks of different intensity eluting after free volume of the column and a well resolved third peak (Figure 6). Fractions corresponding to these peaks were collected and analyzed by SDS-PAGE. The analysis revealed high molecular mass oligomers in the first fraction (Figure 6, inset, lane 1), a mixture of such oligomers and intermediate multimers in the second fraction (Figure 6, inset, lane 2) and a mixture of the dimer and the monomer in the third fraction (Figure 6, inset, lane 3). The first and second fractions were used for further structure/function analysis.

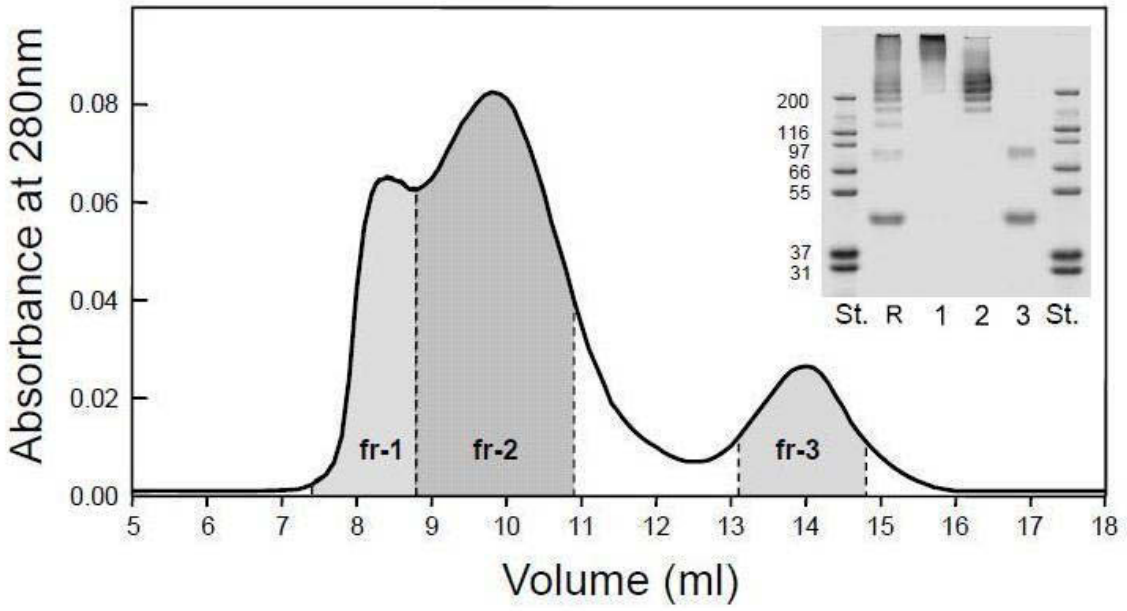

Figure 6: Fractionation of cross-linked Aα221-610 oligomers and SDS-PAGE analysis of individual fractions.

The cross-linking was performed in TBS containing 2 M NaCl using activated factor XIII. The cross-linking reaction was stopped after 30 minutes by adding 10 mM EDTA and the reaction mixture was applied on Superdex 200 column equilibrated with TBS. The inset shows SDS-PAGE analysis of the reaction mixture applied to the column (lane denoted as R), and its individual fractions, fr-1, fr-2, and fr-3 (lanes 1, 2 and 3, respectively). The outer lanes contain protein markers of the indicated molecular masses.

3. Electron microscopy of cross-linked Aα221-610 oligomers

The first and second fractions of soluble cross-linked Aα221-610 oligomers, as well as Aα221-610 monomer, were visualized by electron microscopy after preparation by the method of rotary shadowing. The analysis of monomeric Aα221-610 revealed the presence of small globular structures about 3.8 nm in diameter (Figure 7C). They appeared as individual globules randomly distributed in the field of view. Sometimes similar structures with the same width but about twice this length were also observed. In rotary shadowed preparations of fraction #1 of the cross-linked Aα221-610 oligomers, long linear thin polymers were observed; some large complex structures with multiple branches were also present (Figure 7A). The basic building block of these polymers was a thin filament about 8 nm in width, which is about twice the diameter of individual monomers. The branched network of structures was mainly formed by pair wise lateral aggregation of two of these filaments. In other words, each branch point was made up of two 8 nm filaments and one filament that was about 14 nm, or approximately twice the diameter of each individual filament (Figure 7D). In some cases, the branch points were made up of three 8 nm filaments (shown by arrow in figure 7A). Similar long thin polymers were observed upon analysis of fraction #2 of cross-linked Aα221-610 oligomers (Figure 7B). The only difference was that the structure of fraction #2 contained fewer branched polymers; the polymers were smaller and not as complex in structure as those in fraction #1. Thus, these results suggest that the αC-domains in cross-linked Aα221-610 oligomers are highly ordered forming linear compact structures.

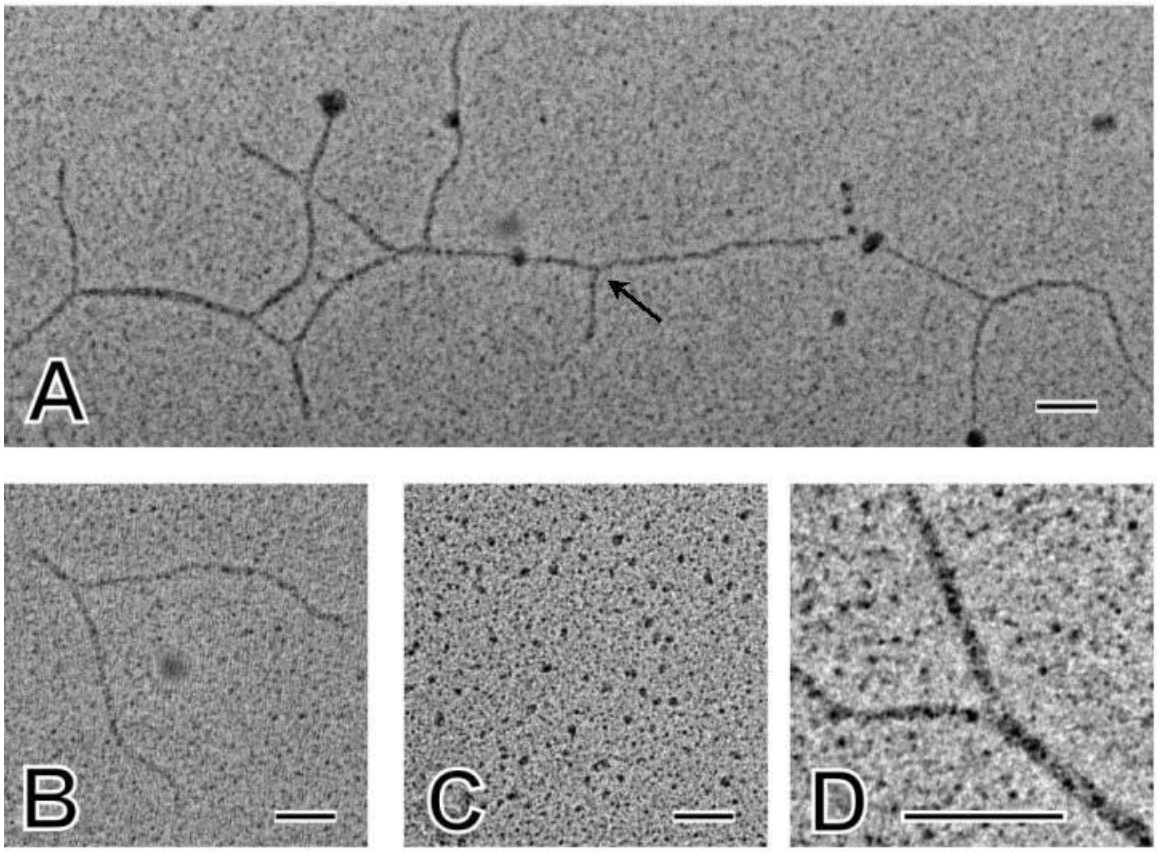

Figure 7: Electron microscopy of rotary-shadowed samples of cross-linked Aα221-610 oligomers.

Panel A shows the structure of cross-linked Aα221-610 oligomers prepared from fraction #1; the structure of those prepared from fraction #2 is shown in panel B; panel C represents samples of the monomeric Aα221-610 fragment; panel D shows enlarged image of a branch point of fraction #1 of cross-linked Aα221-610 oligomers. The bar in all panels indicates 100 nm.

4. Circular dichroism study of cross-linked Aα221-610 oligomers

To characterize the structure of cross-linked Aα221-610 oligomers, circular dichroism (CD) measurements were performed. Visual examination of CD spectrum of such oligomers revealed a well-pronounced negative band at about 217 nm suggesting the presence of significant amount of β-sheet structure (Figure 8, red curve). Analysis of this spectrum using the secondary structure prediction program supplied with the CD instrument revealed the presence of about 43% β-sheets, 12% β-turns and 10% α-helices with only 35% random coil conformation. This spectrum was comparable with that of the preferentially (about 90%) oligomeric Aα392-610 fragment that was purified from the mixture of Aα392-610 oligomers and monomer incubated overnight in TBS (Figure 8, blue curve). In contrast, CD spectrum of the monomeric Aα221-610 fragment showed a weaker band at 217 nm and a dominant negative band at about 200 nm suggesting the presence of substantial amount of random structures in this species (Figure 8, black curve). These results indicate that cross-linked Aα221-610 oligomers contain significant amount of regular structures (mainly β-sheets).

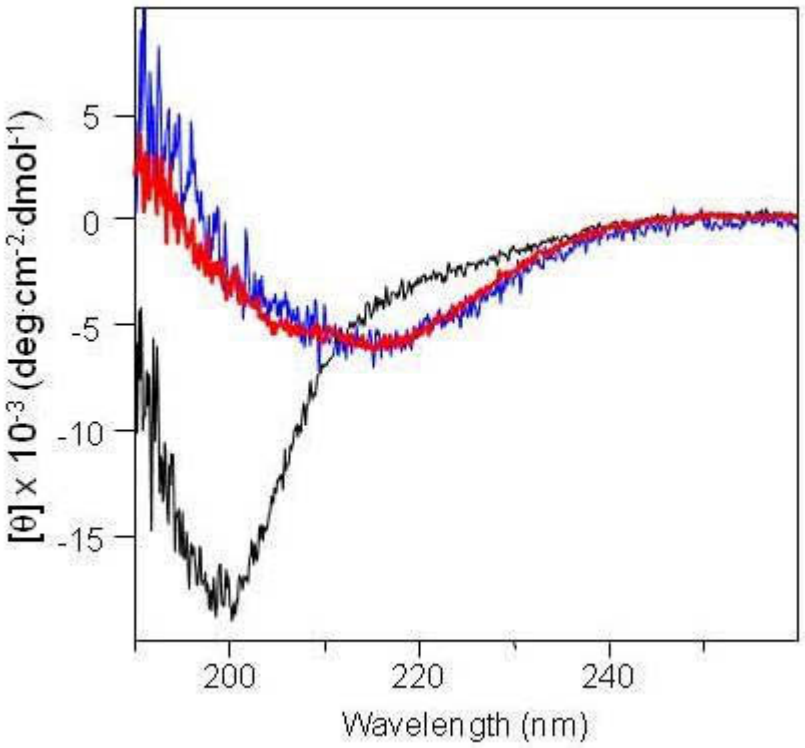

Figure 8: CD spectra of cross-linked Aα221-610 oligomers (red), Aα221-610 monomer (black), and Aα392-610 oligomers (blue).

The experiments were performed in 20 mM Tris, pH 7.4, containing 0.15 M NaCl (TBS); fragment concentrations were 0.5-1.0 mg/mL. All spectra were obtained in 0.01 cm cuvette at 4 ^{o}C.

5. Fluorescence study of cross-linked Aα221-610 oligomers

The folding status and stability of cross-linked Aα221-610 oligomers were tested by fluorescence spectroscopy and compared with those of non-cross-linked Aα221-610 oligomers. First, fluorescence measurements of both species were performed in TBS at 0.05 mg/ml concentration. When heated in the fluorometer while the ratio of fluorescence intensity at 370 nm to that at 330 nm was monitored as a measure of the spectral shift that accompanies unfolding, the cross-linked oligomers exhibited a well-pronounced sigmoidal transition reflecting the unfolding of their compact structure. The midpoint (T_m) of the transition was found to be at 60.7 ± 0.4 ^{0}C (n = 2) (Figure 9A). Upon melting, non-cross-linked oligomeric fraction exhibited similar transition, however, the unfolding was observed at much lower temperature with T_m = 42.5 ± 0.2 ^{0}C (n = 2).

Since oligomerization of Aα221-610 is a reversible process and dilution of the oligomeric fraction to a concentration required for fluorescence study could result in their dissociation, which may lead to lower thermal stability of non-cross-linked oligomers, we tested the distribution of the oligomers and monomers in the non-cross-linked oligomeric fraction by size-exclusion chromatography on Superdex 200. The experiment revealed substantial amount of monomers (about 60%) after one-hour incubation at room temperature in TBS. Thus, the lower stability of the non-cross-linked oligomers could be connected with their dissociation upon experiment. Alternatively, the cross-linking could be responsible for the increased stability of the cross-linked oligomers. To examine the potential for these alternatives, we compared the thermal stability of cross-linked and non-cross-linked Aα221-610 oligomers in TBS containing 2 M NaCl. It was expected that high concentration of NaCl would preserve more non-cross-linked oligomers from

dissociation. Indeed, the size-exclusion chromatography of non-cross-linked oligomers diluted to 0.05 mg/ml, a concentration required for fluorescent study, and incubated in TBS containing 2 M NaCl for 60 min revealed only about 10% monomers in the mixture. In these conditions, the non-cross-linked and cross-linked oligomers unfolded practically in the same temperature ranges as in TBS with very similar T_ms, 42.2 ± 0.6 ^{0}C (n = 2) and 60.2 ± 0.7 ^{0}C (n = 3), respectively (Figure 9B). Thus, the lower stability of non-cross-linked oligomers cannot be explained by their dissociation during the experiment.

Altogether, these experiments indicate that the αC-domain in cross-linked Aα221-610 oligomers is folded into a compact structure, which is more stable than that in non-cross-linked oligomers. They also suggest that the increased thermal stability of the αC-domains in the cross-linked oligomers is mainly connected with their covalent cross-linking by factor XIIIa.

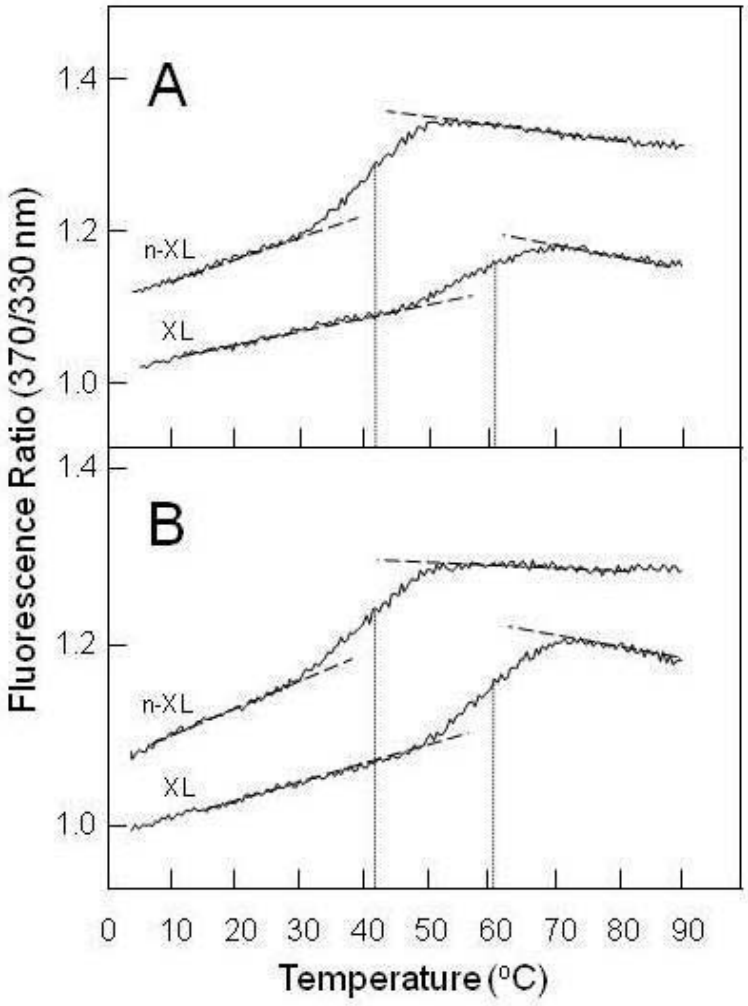

Figure 9: Fluorescence-detected thermal unfolding of cross-linked (XL) and non-cross-linked (n-XL) Aα221-610 oligomers.

Experiments were conducted in 20 mM Tris, pH 7.4, containing 0.15 M NaCl (panel A) and in 20 mM Tris, pH 7.4, containing 2 M NaCl (panel B). The unfolding curves have been arbitrarily shifted along the vertical axis to improve visibility; the dashed straight lines represent linear extrapolations of the values of the fluorescence ratio at 370/330nm before and after transitions to highlight their sigmoidal character; the dotted vertical lines show midpoint temperature (T_m) of the unfolding transitions.

6. ELISA-detected interaction of tPA and plasminogen with cross-linked Aα221-610 oligomers and Aα221-610 monomer

To test the hypothesis that αC-domain cryptic binding sites are exposed in cross-linked Aα221-610 oligomers, we studied the interaction of these oligomers with two αC-domain ligands, tPA and plasminogen, by ELISA. In these experiments, microtiter plate wells were coated with tPA or plasminogen and cross-linked Aα221-610 oligomers, monomeric Aα221-610, or fibrinogen, all at 1 μM concentration, were added to the wells. Since commercially available fibrinogen usually contains small amount of soluble fibrinogen aggregates that may interfere its interaction with tPA and plasminogen, such fibrinogen was additionally purified before conducting these and other binding experiments by size-exclusion chromatography on Superdex 200 column. The bound fragments were detected as described in Materials and Methods. Analysis of the results revealed a prominent binding for cross-linked Aα221-610 oligomers with little or no binding for Aα221-610 monomer although both were added at the same concentration (Figure 10). Fibrinogen used as a control also failed to bind, as expected (Figure 10). Thus, these results support the above mentioned hypothesis.

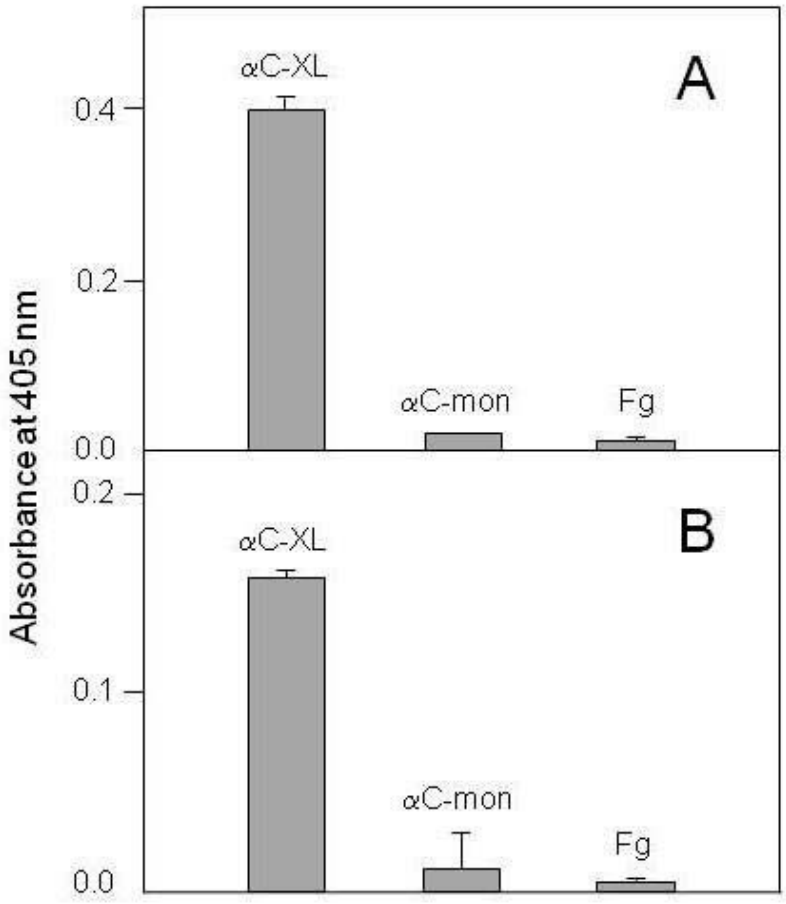

Figure 10: ELISA-detected binding of cross-linked Aα221-610 oligomers, Aα221-610 monomer, and fibrinogen to immobilized plasminogen or tPA.

1 μM of cross-linked Aα221-610 oligomers (αC-XL), Aα221-610 monomer (αC-mon), or fibrinogen (Fg) was added to surface-adsorbed plasminogen (panel A) or tPA (panel B). Bound fragments were detected spectrophotometrically, as described in Materials and Methods. All results are means ± the standard deviation of two independent experiments, each performed in duplicate.

7. Study of the interaction of tPA and plasminogen with cross-linked Aα221-610 oligomers and Aα221-610 monomer by surface plasmon resonance

The results obtained from ELISA were confirmed by SPR experiments. In SPR, plasminogen and tPA were immobilized to the surface of a sensor chip, Aα221-610 monomer, cross-linked Aα221-610 oligomers, or fibrinogen, all at 1 μM, were injected and their association/dissociation was measured in real time. Fibrinogen was additionally purified prior to the experiments, as described above. Between these fragments, only the oligomers exhibited prominent binding while Aα221-610 monomer and fibrinogen failed to bind (Figure 11). The binding was dose-dependent since the SPR signal increased when the oligomers were injected at 2 μM (Figure 11, broken curves). In another SPR experiment, the monomer and oligomers were immobilized onto the surface of a sensor chip and tPA or plasminogen, both at 2 μM concentration, were added. The results showed a prominent binding of tPA and plasminogen only to the cross-linked oligomers while binding to the monomer was negligible (Figure 12). To determine the equilibrium dissociation constant (K_d) for these bindings, tPA or plasminogen were injected at increasing concentrations (Figure 13) and the binding data were analyzed as described in Materials and Methods section. The analysis revealed the K_d values of 440 ± 15 and 458 ± 9 nM for binding of tPA and plasminogen, respectively.

Altogether, the results of ELISA and SPR experiments described above clearly indicate that the tPA- and plasminogen-binding sites are cryptic in fibrinogen and the monomeric Aα221-610 including the αC-domain and are exposed in cross-linked Aα221-610 oligomers.

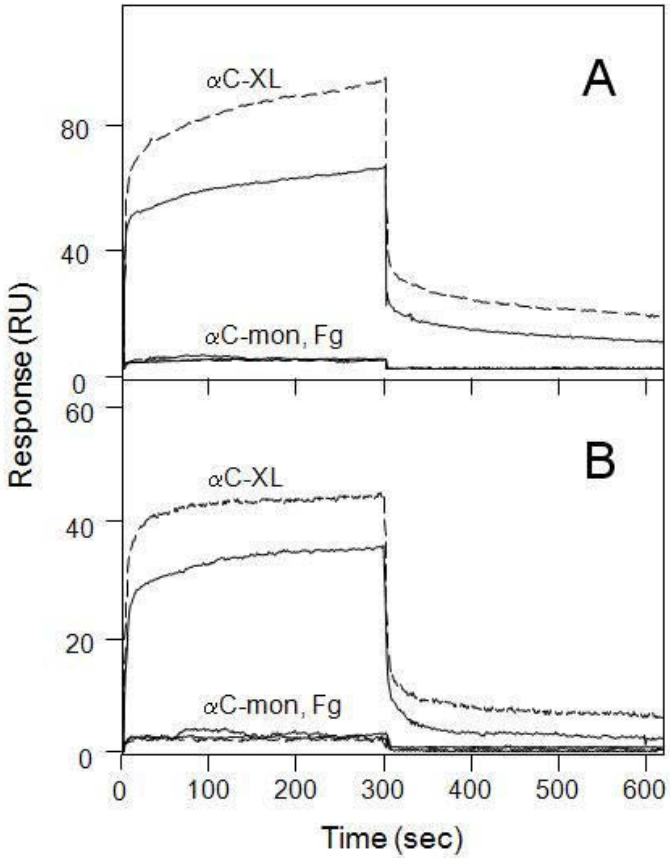

Figure 11: Binding of cross-linked Aα221-610 oligomers and Aα221-610 monomer to immobilized plasminogen or tPA detected by surface plasmon resonance.

Cross-linked Aα221-610 oligomers (αC-XL), Aα221-610 monomer (αC-mon), or fibrinogen (Fg), all at 1 μM, were added to immobilized plasminogen (panel A) or tPA (panel B) and their association/dissociation was monitored in real time (solid curves). Broken curves in both panels show binding of cross-linked Aα221-610 oligomers (αC-XL) or Aα221-610 monomer (αC-mon) both added at 2 μM. Note that the curves for Aα221-610 monomer at both concentrations and for fibrinogen essentially coincide.

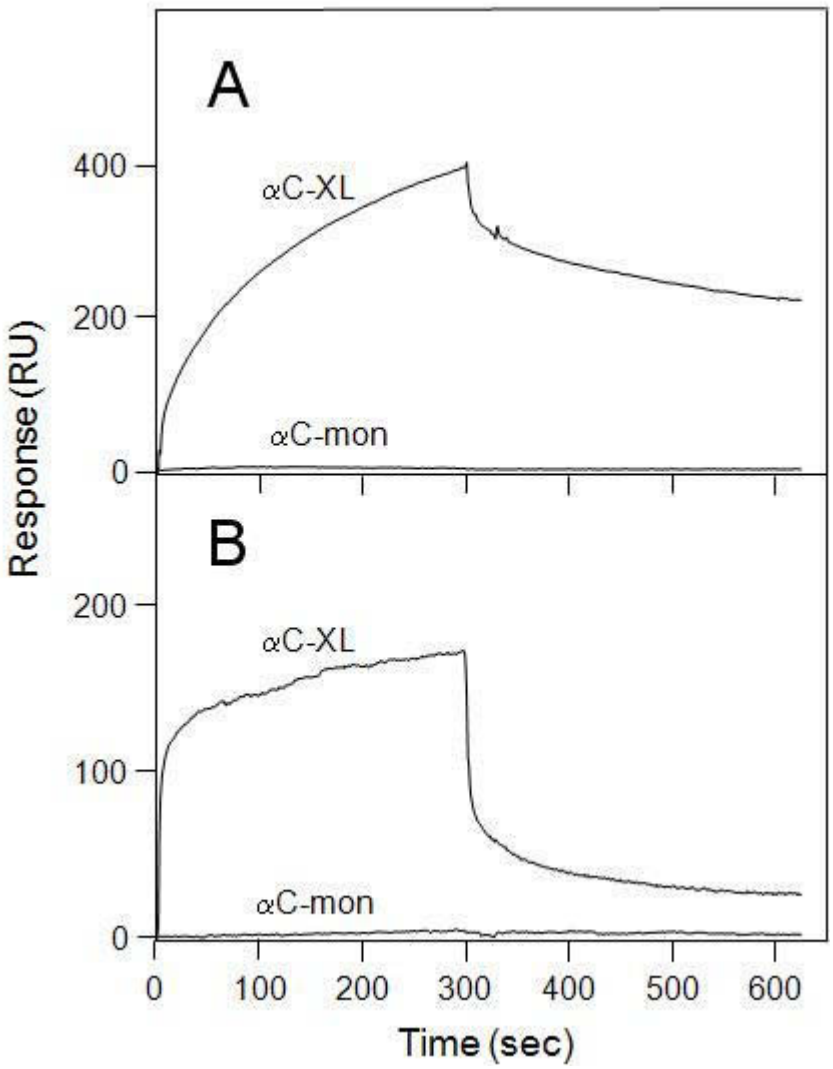

Figure 12: Binding of plasminogen and tPA to immobilized Aα221-610 monomer and cross-linked Aα221-610 oligomers detected by surface plasmon resonance.

Plasminogen (panel A) or tPA (panel B), each at 2 μM, was added to immobilized cross-linked Aα221-610 oligomers (αC-XL) or Aα221-610 monomer (αC-mon) and their association/dissociation was monitored in real time.

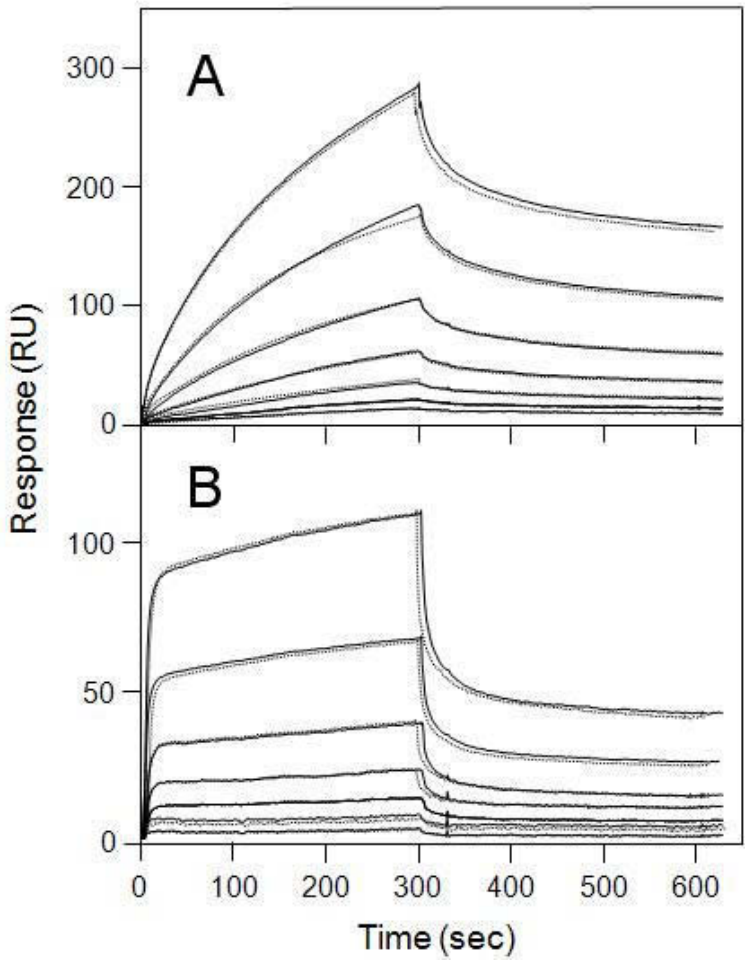

Figure 13: Analysis of the concentration-dependent binding of plasminogen and tPA to cross-linked Aα221-610 oligomers by surface plasmon resonance.

Increasing concentrations of plasminogen (panel A) or tPA (panel B) were added to the immobilized cross-linked oligomers and their association/dissociation was monitored in real time. The concentrations were 16, 32, 63, 125, 250, 500 and 1000 nM, respectively; the dotted curves in both panels represent the best fit of the data using the kinetic analysis of the association/dissociation data (see Materials and Methods).

8. Stimulating effect of cross-linked Aα221-610 oligomers and Aα221-610 monomer on activation of plasminogen by tPA

It is well established that fibrin binds tPA and plasminogen and accelerates dramatically activation of the latter by the former thus promoting fibrinolysis. After confirming that tPA- and plasminogen-binding sites were cryptic in the monomeric Aα221-610 fragment and exposed in cross-linked Aα221-610 oligomers, the stimulating effect of these species on plasminogen activation was tested using chromogenic substrate assay. In this assay, plasminogen was activated by tPA and newly generated plasmin was detected by measuring its proteolytic activity towards specific chromogenic substrate S-2251. The experiments revealed a very dramatic difference in the activation of plasminogen in the presence of the monomer and oligomers (Figure 14). The cross-linked oligomers exhibited a prominent stimulating effect while that of the monomer was very low. Freshly purified fibrinogen used as a control in the assay also exhibited a very low stimulation. The previously tested cross-linked Aα221-610 monomers were prepared following the procedure described earlier [44]. Their stimulating effect was then compared with that of cross-linked Aα221-610 oligomers. Although the cross-linked monomers stimulated plasminogen activation, their effect was lower than that of the cross-linked oligomers. The observed superior stimulating effect of cross-linked Aα221-610 oligomers indicates that the αC-domains adopt physiologically active conformation only upon their oligomerization. This further confirms the hypothesis that polymerization of the αC-domains result in the exposure of their cryptic binding sites.

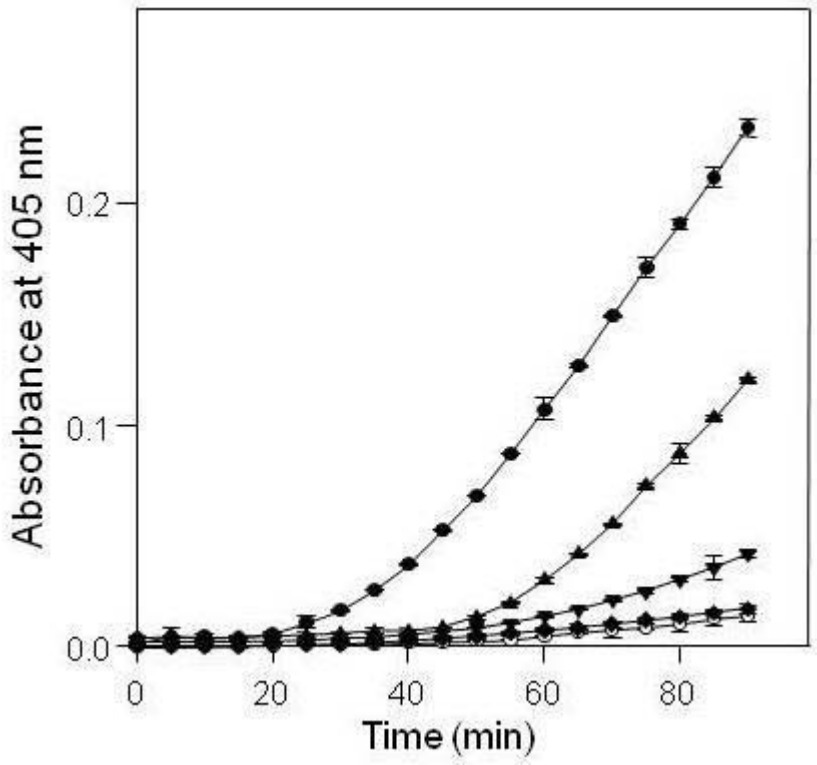

Figure 14: Stimulating effect of various forms of Aα221-610 fragment on activation of plasminogen by tPA.

Stimulating effect of cross-linked Aα221-610 oligomers (circles), cross-linked Aα221-610 monomers (triangles up), Aα221-610 monomer (triangles down), and fibrinogen (diamonds) was measured by hydrolysis of chromogenic substrate S-2251 with newly formed plasmin as described in Materials and Methods; the activation of plasminogen in the absence of stimulators is shown by empty circles. Each point represents the mean ± S.D. of 3 independent experiments.

V. DISCUSSION

According to the current hypothesis, upon conversion of fibrinogen into fibrin, the αC-domains switch from intra- to intermolecular interaction to form αC-domain polymers and such a switch is connected with conformational changes that result in physiologically active conformations of the αC-domains in fibrin αC polymers [30, 45, 57]. While the structure of the individual fibrinogen αC-domain has been established, little is known about their structure and function in polymeric fibrin. The major problems in studying the structure and interaction of fibrin αC-domain polymers are the complexity of fibrin structure and the presence of multiple domains some of which duplicate the activity of the αC-domain. These polymers, in contrast to some other fibrin(ogen) domains or regions, cannot be prepared by limited proteolysis of fibrin due to their rapid degradation into smaller fragments. In the present study, we overcame these problems by preparing a soluble model of αC-domain polymers, which mimics the structure and properties of the αC-domains in fibrin, using the recombinant Aα221-610 fragment corresponding to the fibrinogen αC region. The study revealed that in this model, Aα221-610 fragment forms ordered linear oligomers that are stable in solution and contain compact structure whose thermal stability is similar to that of the αC-domains in fibrin. Furthermore, in contrast to the monomeric αC-domain, such oligomers exhibited a prominent binding to plasminogen and tPA supporting our hypothesis that αC-domain binding sites become exposed upon formation of αC polymers in fibrin.

Previous electron microscopy study of the proteolytically prepared bovine fibrinogen Aα223-539 fragment, containing the truncated αC-domain and the αC-

connector, revealed that this fragment forms linear, ordered oligomers [21]. This finding suggested that such oligomers may mimic the arrangement of the αC-domains in fibrin. However, preparation of this fragment was complicated by a very low yield due to high susceptibility of the αC-domains to proteolysis; in addition, the C-terminal portion of the αC-domain in the resulting fragment was missing [21]. To circumvent these limitations, recombinant bovine Aα224-568 fragment containing the full-length αC-domain and αC-connector and its human analog, the Aα221-610 fragment, were prepared [13]. While such fragments exhibited some ordered oligomers under electron microscope, those oligomers were not observed in solution where the fragments were preferentially monomeric [59]. To solve this problem, the bAα224-568 and the Aα221-610 fragments were covalently cross-linked with factor XIIIa to make soluble oligomers [59]. Such oligomers were stable, i.e. did not dissociate in solution, however, electron microscopy revealed that they were neither linear nor ordered [59], most probably because both fragments were mostly in monomeric state at the time of cross-linking and the cross-linking occurred in a random manner. These results suggested that the structure of those oligomers does not mimic that of αC polymers in fibrin. Thus, previous attempts to prepare a stable soluble model of αC-domain polymers failed, however, they provided valuable information that prompted us to further search for a more adequate soluble model of fibrin αC polymers that would be stable in solution and highly ordered.

Our search for such a model was facilitated by a recent finding, which revealed that the recombinant αC-domain, as well as its N-terminal sub-domain, forms ordered oligomers in a concentration-dependent and reversible manner [34, 35]. Another finding that the αC-domain interacts with the αC-connector [60] suggested that such interaction

may further promote formation of oligomers by the full-length αC region and provide a proper alignment of these portions in such oligomers for their more efficient cross-linking with factor XIIIa. Therefore, in the present study, we prepared the recombinant Aα221-610 fragment corresponding to this region, confirmed that it forms oligomers, purified such oligomers, and then stabilized them by covalent cross-linking with factor XIIIa to prevent their dissociation in solution.

Several lines of evidence indicate that prepared cross-linked Aα221-610 oligomers are highly ordered. First, oligomerization of Aα221-610 was concentration-dependent and reversible indicating highly specific interaction between αC-domains in the oligomers. Second, relatively rapid cross-linking of the oligomers with factor XIIIa compared to that of the Aα221-610 monomer further confirmed ordered arrangement of the αC-connectors and αC-domains in the oligomers. Third, electron microscopy revealed that the oligomers appeared as well organized, almost linear arrays with the width of two monomeric molecules. Finally, spectral studies confirmed that the αC-domains in such oligomers were folded into compact cooperative units with a high content of regular structures and their thermal stability was comparable with that of the αC-domains in fibrin [10, 12, 61]. Thus, such highly ordered and reversible oligomerization of isolated Aα221-610 suggests that in fibrin the corresponding αC regions form αC polymers in a similar manner. This implies that cross-linked Aα221-610 oligomers mimic fibrin αC polymers.

Electron microscopy images of cross-linked Aα221-610 oligomers indicate that besides individual linear arrays they also contain branched oligomers. Analysis of the width of such oligomers revealed that some of the arrays have the same thickness before

branching point as individual non-branched oligomers, while others are twice thicker. This suggests at least two mechanism of branching; one mechanism may involve cross-linking of individual oligomers through their ends while another one may occur through lateral association of two individual oligomers. The first type of branching could be the result of random cross-linking through unoccupied reactive Lys and Gln residues while the second one may require specific lateral interaction between individual αC oligomers. Whether such specific interaction and branching could also occur between αC polymers in fibrin, in which they should be located close to each other, remains to be clarified.

Our CD study indicates that individual αC-domains in cross-linked Aα221-610 oligomers are also highly ordered. While Aα221-610 monomer exhibited substantial amount of unordered structure, the content of such structures in the oligomers did not exceed 35%. The increase in regular structure content upon oligomerization is, most probably, connected with folding of the C-terminal sub-domains, which was shown earlier to adopt folded conformation (preferentially consisting of β-sheet structures) in oligomers [34]. However, this sub-domain and the N-terminal sub-domain together represent no more than a half of the Aα221-610 fragment (αC region) while another half belongs to the αC-connector, which is considered to be flexible and unordered [13, 29]. The present study thus suggests that the αC-connector or its portion(s) may also be ordered in cross-linked Aα221-610 oligomers. This is in agreement with the results of fluorescence experiments that were obtained by monitoring fluorescence of Trp residues upon unfolding of such oligomers. Although monitoring of fluorescence of Trp residues located in the αC-connector did not reveal any sigmoidal transition upon unfolding of Aα221-610 monomer (not shown), fluorescence of these Trp residues was very

responsive to unfolding in the oligomers (Figure 9). This suggests that probably all or part of the Trp residues were in ordered environment in the oligomers. Thus, the results of the present study suggest that the αC-connector or its portion(s) adopt regular conformation upon formation of αC polymers. This is in agreement with the previous finding that conversion of fibrinogen into fibrin is accompanied by a significant increase of the β-sheet structure that was speculated to occur due to interaction between C-terminal parts of the α chains in polymeric fibrin [62, 63].

Having developed a model mimicking fibrin αC polymers (cross-linked Aα221-610 oligomers), we used this model to test our hypothesis that polymerization of the αC-domains in fibrin results in the exposure of their multiple binding sites. Since it was established that fibrin(ogen) αC-domains interact with plasminogen and tPA [44], these two ligands were used as molecular probes for testing such exposure. Our ELISA and SPR experiments revealed that these ligands did not interact with the monomeric Aα221-610 fragment kept in solution. In SPR, no interaction was also observed with monomeric Aα221-610 immobilized on the surface of a sensor chip. In contrast, these ligands exhibited a prominent binding to cross-linked Aα221-610 oligomers supporting the above hypothesis. Moreover, these oligomers exhibited a prominent stimulating effect on activation of plasminogen by tPA while that of Aα221-610 monomer was very low further supporting the above hypothesis. Altogether, these results indicate that the αC-domains adopt physiologically active conformation only upon their polymerization in fibrin.

In summary, in this study we prepared soluble Aα221-610 oligomers containing the αC-domains and stabilized their structure by covalent cross-linking with factor XIIIa.

Physico-chemical and biochemical studies of these oligomers revealed that their oligomerization occurs through highly specific interactions between monomeric units and results in formation of compact ordered linear arrays that most probably reflect the structure of αC polymers in fibrin. They also confirmed our hypothesis that the αC-domains adopt physiologically active conformation in such polymers. Thus, cross-linked Aα221-610 oligomers represent a simple soluble model that mimics structural and functional properties of the αC-domain in fibrin αC polymers. This model can be used to further study the structure and function of fibrin αC-domains.

VI. REFERENCES:

1. Henschen, A., and McDonagh, J. (1986) Fibrinogen, fibrin and factor XIII. in Blood Coagulation (Zwaal, R. F. A., and Hemker, H. C., Eds.) pp 171-241, Elsievier Science Publishers, Amsterdam.

2. Clark, R. A. F. (2001) Fibrin and wound healing. *Ann. N.Y. Acad.* Sci. 936: 355-367.

3. Belkin, A. M., Tsurupa, G., Zemskov, E., Veklich, Y., Weisel, J. W., and Medved, L. (2005) Transglutaminase-mediated oligomerization of the fibrin(ogen) αC-domains promotes integrin-dependent cell adhesion and signaling. *Blood* 105: 3561-3568.

4. Collen, D. (1999) The plasminogen (fibrinolytic) system. *Thromb. Haemostasis* 82: 259-270.

5. Ugarova, T. P., and Yakubenko, V. P. (2001) Recognition of fibrinogen by leukocyte integrins. *Ann. N.Y. Acad. Sci.* 936: 368-385.

6. Martinez, J., Ferber, A., Bach, T. L., and Yaen, C. H. (2001) Interaction of fibrin with VE-cadherin. *Ann. N.Y Acad. Sci.* 936: 386-405.

7. Medved, L., and Weisel, J. W. (2009) Recommendations for nomenclature on fibrinogen and fibrin. *Thromb. Haemostasis* 7: 355-359.

8. Medved, L., Tsurupa, G., and Yakovlev, S. (2001) Corformational changes upon conversion of fibrinogen into fibrin. The mechanisms of exposure of cryptic sites. *Ann. N.Y. Acad. Sci.* 936: 185-204.

9. Doolittle, R. F. (1984) Fibrinogen and fibrin. *Annu. Rev. Biochem.* 53: 195-229.

10. Privalov, P. L., and Medved, L. V. (1982) Domains in the fibrinogen molecule. *J. Mol. Biol.* 159: 665-683.

11. Medved, L., Litvinovich, S., Ugarova, T., Matsuka, Y., and Ingham, K. (1997) Domain structure and functional activity of the recombinant human fibrinogen γ-module. *Biochemistry* 36: 4685-4693.

12. Medved, L. V., Gorkun, O. V., and Privalov, P. L. (1983) Structural organization of C-terminal parts of fibrinogen Aα-chains. *FEBS Lett.* 160: 291-295.

13. Tsurupa, G., Tsonev, L., and Medved, L. (2002) Structural organization of the fibrin(ogen) αC-domain. *Biochemistry* 41: 6449-6459.

14. Gorlatov, S., and Medved, L. (2002) Interaction of fibrin(ogen) with the endothelial cell receptor VE-cadherin: mapping of the receptor-binding site in the NH_2-terminal portions of the fibrin β chains. *Biochemistry* 41: 4107-4116.

15. Hall, C., and Slayter, H. (1959) The fibrinogen molecule: its size, shape and mode of polymerization. *J. Biophys. Biochem. Cytol.* 5: 11-15.

16. Doolittle, R. F. (1973) Structural aspects of the fibrinogen to fibrin conversion. *Adv. Protein Chem.* 27: 1-109.

17. Weisel, J. W., Stauffacher, C. V., Bullitt, E., and Cohen, C. (1985) A model for fibrinogen: domains and sequence. *Science* 230: 1388-1391.

18. Weisel, J. W. (2005) Fibrinogen and fibrin. *Adv. Protein chem.* 70: 247-299.

19. Erickson, H. P., and Fowler, W. E. (1983) Electron microscopy of fibrinogen, its plasmic fragmens and small polymers. *Ann. N.Y. Acad. Sci.* 408: 146-163.

20. Pizzo, S. V., Schwartz, M. L., Hill, R. L., and McKee, P. A. (1972) The effect of plasmin on the subunit structure of human fibrinogen. *J. Biol. Chem.* 247: 636-645.

21. Veklich, Y. I., Gorkun, O. V., Medved, L. V., Nieuwenhuizen, W., and Weisel, J. W. (1993) Carboxyl-terminal portions of the α chains of fibrinogen and fibrin. Localization by electron microscopy and the effects of isolated αC fragments on polymerization. *J. Biol. Chem.* 268: 13577-13585.

22. Rudchenko, S., Trakht, I., and Sobel, J. H. (1996) Comparative structural and functional features of the human fibrinogen αC domain and the isolated αC fragment: characterization using monoclonal antibodies to defined COOH terminal Aα chain regions. *J. Biol. Chem.* 271: 2523-2530.

23. Madrazo, J., Brown, J. H., Litvinovich, S., Dominguez, R., Yakovlev, S., Medved, L., and Cohen, C. (2001) Crystal structure of the central region of

bovine fibrinogen (E5 fragment) at 1.4-Å resolution. *Proc. Natl. Acad. Sci.* 98: 11967-11972.

24. Spraggon, G., Everse, S. J., and Doolittle, R. F. (1997) Crystal structures of fragment D from human fibrinogen and its cross-linked counterpart from fibrin. *Nature* 389: 455-462.

25. Yee, V. C., Pratt, K. P., Cote, H. C., Trong, I. L., Chung, D. W., Davie, E. W., Stenkamp, R. E., and Teller, D. C. (1997) Crystal structure of a 30 kDa C-terminal fragment from the γ chain of human fibrinogen. *Structure* 5: 125-138.

26. Brown, J. H., Volkmann, N., Jun, G., Henschen-Edman, A. H., and Cohen, C. (2000) The crystal structure of modified bovine fibrinogen. *Proc. Natl. Acad. Sci.* 97: 85-90.

27. Kollman, J. M., Pandi, L., Sawaya, M. R., Riley, M., and Doolittle, R. F. (2009) Crystal structure of human fibrinogen. *Biochemistry* 48: 3877-3886.

28. Doolittle, R. F., Yang, Z., and Mochalkin, I. (2001) Crystal structure studies on fibrinogen and fibrin. *Ann. N.Y. Acad. Sci.* 936: 31-43.

29. Weisel, J., W., and Medved, L. (2001) The structure and function of the αC-domains of fibrinogen. *Ann. N.Y. Acad. Sci.* 936: 312-327.

30. Medved, L. V., Gorkun, O. V., Manyakov, V. F., and Belitser, V. A. (1985) The role of fibrinogen αC-domains in the fibrin assembly process. *FEBS Lett.* 181: 109-112.

31. Mosesson, M. W., Siebenlist, K. R., and Meh, D. A. (2001) The structure and biological features of fibrinogen and fibrin. *Ann. N.Y. Acad. Sci.* 936: 11-30.

32. Medved, L., and Nieuwenhuized, W. (2003) Molecular mechanisms of initiation of fibrinolysis by fibrin. *Thromb. Haemostasis* 89: 409-419.

33. Doolittle, R. F., and Kollman, J. M. (2006) Natively unfolded regions of the vertebrate fibrinogen molecule. *Proteins* 63: 391-397.

34. Tsurupa, G., Hantgan, R. R., Burton, A. R., Pechik, I., Tjandra, N., and Medved, L. (2009) Structure, stability and interaction of the fibrin(ogen) αC-domains. *Biochemistry* 48: 12191-12201.

35. Burton, A. R., Tsurupa, G., Hantgan, R. R., Tjandra, N., and Medved, L. (2007) NMR solution structure, stability, and interaction of the recombinant bovine fibrinogen αC-domain fragment. *Biochemistry* 46: 8550-8560.

36. Matsuka, Y. V., Medved, L. V., Migliorini, M. M., and Ingham, K. C. (1996) Factor XIIIa catalyzed cross-linking of recombinant αC fragments of human fibrinogen. *Biochemistry* 35: 5810-5816.

37. Cottrell, B. A., Strong, D. D., Watt, K. W., and Doolittle, R. F. (1979) Amino acid sequence studies on the α chain of human fibrinogen. Exact location of cross-linking acceptor sites. *Biochemistry* 18: 5405-5410.

38. Corcoran, D. H., Ferguson, E. W., Fretto, L. J., and Mckee, P.A. (1980) Localization of a cross-link donor site in the α-chain of human fibrin. *Thromb. Res.* 19: 883-888.

39. Shen, L. L., McDonagh, R. P., McDonagh, J., and Hermans, J. (1977) Early events in the plasmin digestion of fibrinogen and fibrin. Effects of plasmin on fibrin polymerization. *J. Biol. Chem.* 252: 6184-6189.

40. Gorkun, O. V., Veklich, Y. I., Medved, L. V., Heneschen, A. H., and Weisel, J. W. (1994) Role of the αC domains of fibrin in clot formation. *Biochemistry* 33: 6986-6997.

41. Credo, R. B., Curtis, C. G., and Lorand, L. (1981) α-chain domain of fibrinogen controls generation of fibrinoligase (coagulation factor XIIIa). Calcium ion regulatory aspects. *Biochemistry* 20: 3770-3778.

42. Cheresh, D. A., Berliner, S. A., Vicente, V., and Ruggeri, Z. M. (1989) Recognition of distinct adhesive sites on fibrinogen by related integrins on platelets and endothelial cells. *Cell* 58: 945-953.

43. Corbett, S. A., Lee, L., Wilson, C. L., and Schwarzbauer, J. E. (1997) Covalent cross-linking of fibronection to fibrin is required for maximal cell adhesion to a fibronectin-fibrin matrix. *J. Biol. Chem.* 272: 24999-25005.

44. Tsurupa, G., and Medved, L. (2001) Identification and characterization of novel tPA and plasminogen binding sites within fibrin(ogen) αC-domains. *Biochemistry* 40: 801-808.

45. Tsurupa, G., Yakovlev, S., McKee, P., and Medved, L. (2010) Noncovalent interaction of α_2-antiplasmin with fibrin(ogen): localization of α_2-antiplasmin-binding sites. *Biochemistry* 49: 7643-7651.

46. Holm, B., Brosstad, F., Kierulf, P., and Godal, H. C. (1985) Polymerization properties of two normally circulating fibrinogens, HMW and LMW. Evidence that the COOH-terminal end of the α-chain if of importance for fibrin polymerization. *Thromb. Res.* 39: 595-606.

47. Weisel, J. W., and Papsun, D. M. (1987) Involvement of the COOH-terminal portion of the α-chain of fibrin in the branching of fibers to form a clot. *Thromb. Res.* 47: 155-163.

48. Collet, J. P., Moen, J. L., Veklich, Y. I., Gorkun, O. V., Lord, S. T., Montalescot, G., and Weisel, J. W. (2005) The αC-domains of fibrinogen affect the structure of the fibrin clot, its physical properties, and its susceptibility to fibrinolysis. *Blood* 106: 3824-3830.

49. Lijnen, H. R., Soria, J., Soria, C., Collen, D., and Caen, J. P. (1984) Dysfibrinogenemia (fibrinogen dusard) associated with impaired fibrin-enhanced plasminogen activation. *Thromb. Haemostasis* 51: 108-109

50. Koopman, J., Haverkate, F., Grimbergen, J., Egbring, R., and Lord, S. T. (1992) Fibrinogen Marburg: a homozygous case of dysfibrinogenemia, lacking amino acids Aα 461-610 (Lys 461 AAA--> stop TAA). *Blood* 80: 1972-1979.

51. Koopman, J., Haverkate, F., Grimbergen, J., Lord, S. T., Mosesson, M. W., DiOrio, J. P., Siebenlist, K. S., Legrand, C., Soria, J., and Soria, C. (1993) Molecular basis for fibrinogen Dusart (Aα 554 Arg-->Cys) and its association with abnormal fibrin polymerization and thrombophilia. *J. Clin. Invest.* 91: 1637-1643.

52. Benson, M. D., Liepnieks, J., Uemichi, T., Wheeler, G., and Correa, R. (1993) Hereditary renal amyloidosis associated with a mutant fibrinogen α-chain. *Nat. Genet.* 3: 252-255.

53. Uemichi, T., Liepnieks, J. J., and Benson, M. D. (1994) Hereditary renal amyloidosis with a novel variant fibrinogen. *J. Clin. Invest.* 93: 731-736.

54. Uemichi, T., Liepnieks, J. J., Yamada, T., Gertz, M. A., Bang, N., and Benson, M. D. (1996) A frame shift mutation in the fibrinogen Aα chain gene in a kindred with renal amyloidosis. *Blood* 87: 4197-4203.

55. Hamidi Asl, L., Liepnieks, J. J., Uemichi, T., Rebibou, J. M., Justrabo, E., Droz, D., Mousson, C., Chalopin, J. M., Benson, M. D., Delpech, M., and Grateau, G. (1997) Renal amyloidosis with a frame shift mutation in fibrinogen Aα-chain gene producing a novel amyloid protein. *Blood* 90: 4799-4805.

56. Makogonenko, E., Tsurupa, G., Ingham, K., and Medved, L. (2002) Interaction of fibrin(ogen) with fibronection: further characterization and localizatin of the fibronection-binding site. *Biochemistry* 41: 7907-7913.

57. Tsurupa, G., Ho-Tin-Noe, B., Algles-Cano, E., and Medved, L. (2003) Identification and characterization of novel lysine-dependent apolipoprotein(a)-binding sites in fibrin(ogen) αC-domains. *J. Biol. Chem.* 278: 37154-37159.

58. Yang, J. T., Wu, C. S. and Martinez, H. M. (1986) Calculation of protein conformation from circular dichroism. *Methods Enzymol.* 130: 208-269.

59. Tsurupa, G., Veklich, Y., Hantgan, R., Belkin, A. M., Weisel, J. W., and Medved, L. (2004) Do the isolated fibrinogen αC-domains form ordered oligomers? *Biophys. Chem.* 112: 257-266.

60. Litvinov, R. I., Yakovlev, S., Tsurupa, G., Gorkun, O. V., Medved, L., and Weisel, J. W. (2007) Direct evidence for specific interactions of the fibrinogen αC-domains with the central E region and with each other. *Biochemistry* 46: 9133-9142.

61. Mihalyi, E. (2004) Review of some unusual effects of calcium binding to fibrinogen. *Biophys. Chem.* 112: 131-140.

62. Marx, J., Hudry-Clergeon, G., Capet-Antonini, F., and Bernard, L. (1979) Laser raman spectroscopy study of bovine fibrinogen and fibrin. *Biochim. Biophys. Acta.* 578: 107-115.

63. Hudry-Clergeon, G., Freyssinet, J., Torbet, J., and Marx, J. (1983) Orientation of fibrin in strong magnetic fields. *Ann. N.Y. Acad. Sci.* 408: 380-387.